

1 **Seasonal variation of mercury concentration of ancient olive**
2 **groves of Lebanon.**

3

4 Nagham Tabaja^{1,2,3}, David Amouroux⁴, Lamis Chalak², François Fourel⁵, Emmanuel Tessier⁴,
5 Ihab Jomaa⁶, Milad El Riachy⁷, Ilham Bentaleb¹

6

7 ¹ ISEM, Univ Montpellier, CNRS, IRD, Montpellier, France

8 ² Faculty of Agronomy, Plant Production Department, The Lebanese University, Dekwaneh, Lebanon

9 ³ Plateforme de Recherche et d'Analyses en Sciences de l'Environnement (PRASE), Ecole Doctorale de Sciences et
10 Technologie, Université Libanaise, Hadath, Liban

11 ⁴ Université de Pau et des Pays de l'Adour, E2S/UPPA, CNRS, Institut des Sciences Analytiques et de Physico-Chimie
12 pour l'Environnement et les Matériaux (IPREM), PAU, France

13 ⁵ UMR CNRS 5023 LEHNA, Université Claude Bernard Lyon 1, Villeurbanne, France

14 ⁶ Department of Irrigation and Agrometeorology, Lebanese Agricultural Research Institute (LARI), P.O. box 287,
15 Zahle, Lebanon

16 ⁷ Department of Olive and Olive Oil, Lebanese Agricultural Research Institute (LARI), P.O. box 287, Zahle, Lebanon

17

18 *Correspondence to:* Ilham Bentaleb (Email: ilham.bentaleb@umontpellier.fr, Tel: +33(0) 6 38 61 57 69)

19

20

21 **Abstract.** This study ~~aimed to investigate~~ **investigates** the seasonality of the mercury (Hg) concentration of olive trees
22 foliage, an iconic tree of the Mediterranean basin. Hg concentrations of foliage, stems, soil surface, and litter were
23 analyzed on monthly basis in ancient olive trees growing in two groves in Lebanon, Bchaaleh and Kawkaba (1300
24 and 672 m.a.s.l respectively). A significantly lower concentration was registered in stems (~7-9 ng/g) with respect to
25 foliage (~35-48 ng/g) in both sites with the highest foliage Hg concentration in late winter-early spring and the lowest
26 in summer. It is noteworthy that olive fruits also have low Hg concentration (~7-11 ng/g). The soil has the highest Hg
27 content (~62-129 ng/g) likely inherited through the cumulated litter biomass (~ 63-76 ng/g). A good covariation
28 observed between our foliage Hg time-series analysis and those of atmospheric Hg concentrations available for
29 southern Italy in the western Mediterranean basin confirms that mercury pollution can be studied through olive trees.
30 ~~More precisely,~~ Spring sampling is recommended if the objective is to assess the tree's susceptibility to Hg uptake.
31 Our study draws an adequate baseline for Eastern Mediterranean and **the** region with similar climatic inventories on
32 Hg vegetation uptake. **In addition to being a baseline to** new studies on olive trees in the Mediterranean to reconstruct
33 regional Hg pollution concentrations in the past and present.

34 **Keywords:** Eastern Mediterranean, ancient groves, *Olea europaea* L., mercury pollution, plant tissues, soil and litter

35 **Introduction**

36
37 Mercury (Hg) is among the most widely distributed potentially toxic metals polluting the Earth (Briffa et al. 2020). It
38 is found as all heavy metals naturally on the Earth's crust reservoir and in the atmosphere through the natural long-
39 term Hg biogeochemical cycle (i.e., volcanic activities, geological weathering). This metal is easily modified into
40 several oxidation states and it can also be spread through many ecosystems (Boening 2000). The natural Hg cycle has
41 been modified due to anthropogenic activities (i.e., mining, smelting, soil erosion due to deforestation, gold extraction,
42 agriculture-fertilizers, manure) (Patra and Sharma 2000). Among natural and anthropogenic Hg emissions, inorganic
43 elemental Hg (Hg(0)) is the most dominant chemical form. It is primarily transferred through the atmosphere by air
44 mass movement and can undergo long-range transport. Because of its high volatility and susceptibility to oxidation,
45 elemental Hg(0) is the predominant form of Hg in the atmosphere that can be accumulated into foliage. This highly
46 diffusive Hg can easily pass biological barriers (i.e. cell membranes, foliage, skin). Mercury has three oxidation states,
47 namely, Hg(0) (elemental mercury), Hg(I) (mercurous), or Hg(II) (mercuric), although Hg(I) mercurous form is not
48 stable under typical environmental conditions and, therefore, is rarely observed. It is likely that the Hg(II) high binding
49 affinities bind covalently with organic groups (Du and Fang, 1983; Clarkson and Magos 2006; Pleijel et al., 2021).
50 The exchange of Hg between the soil and plants is not stable and is variable dependent (e.g. cation-exchange capacity,
51 soil pH, soil aeration, and plant species) (Patra and Sharma 2000). Forests are known to act as a sink of atmospheric
52 Hg. Plant foliage takes up of Hg deposited on leaf surfaces through the stomata (i.e. Leaf gas exchange) and leaf
53 cuticles (Hanson et al. 1995; Jiskra et al. 2018; Li et al. 2017; Lodenius et al. 2003; Maillard et al. 2016; Rea et al.
54 2002; Yanai et al. 2020) where it accumulates with minimal mobility and small portions released back into the
55 atmosphere or transferred to other plant organs (Cavallini et al. 1999; Hanson et al. 1995; Li et al. 2017; Lodenius et
56 al. 2003; Schwesig and Krebs 2003). All together these authors contributed to highlight the dynamic role of the foliar
57 surfaces in terrestrial forest landscapes acting as a source or sink dependent on the magnitude of current Hg

58 concentrations. Hanson et al. (1995) suggested a species-specific compensation concentrations (or compensation
59 points) for Hg deposition.

60 Hg is redistributed to the forest floor through litter and throughfall and hence passes to the soil (Rea et al. 1996). The
61 Hg input through the litter is greater than the input from that of the wet deposition (Wang et al., 2016). Litter has been
62 estimated to constitute 30 to 60 % of the Hg atmospheric deposition in Europe and North America forests (Rea et al.
63 1996; Blackwell and Driscoll 2015; Zhou et al. 2018). According to Wright et al., (2016) the litter Hg is the dominant
64 pathway in forests where it contributes 53 to 90 % of the dry deposition to the forest. In terrestrial ecosystem, ~~soil as~~
65 ~~part of the geological reservoir has naturally the highest Hg reservoir~~ **soils have the highest Hg reservoir** (Obrist et al.,
66 2018; O'Connor et al., 2019) followed by trees (Yang et al., 2018). This Hg is provided by natural geological sources
67 and natural events such as forest fires, volcanic eruptions (Ermolin et al. 2018; Obrist et al. 2018; O'Connor et al.
68 2019) and anthropogenic sources (UNEP, 2019). Though variable from year to year, Hg emission to the atmosphere
69 from biomass burning is considered as an important driver of the global Hg biogeochemical cycle (Friedli et al., 2009;
70 De Simone et al., 2015; McLagan et al., 2021; Dastoor et al., 2022). Soil can also release Hg to the atmosphere (Luo
71 et al., 2016; Assad, 2017; Yang et al., 2018; Schneider et al., 2019; Gworek et al., 2020; Pleijel et al., 2021) and also
72 behave as a source of Hg to the plants. Hg of the soil is taken up by the roots along with the water, it is translocated
73 to other parts (ie. Stems, Leaves) of the plant using the xylem sap (Bishop et al., 1998; Li et al., 2017). This pathway
74 ~~have~~ **has** been described on several plant species in Hg contaminated sites (Assad et al. 2017). Trees are hence
75 considered as important drivers of Hg exchange between the atmosphere and the soil (Yang et al. 2018). The recent
76 studies on Hg uptake by vegetation have highlighted the importance of the role of different parameters as vapor
77 pressure deficit, soil water content, climatic conditions, date of sampling, leaf mass area, tree functional groups,
78 stomatal conductance, affecting potentially the root uptake of Hg dissolved in soil water and the absorption rate via
79 stomata and eventually the Hg leaf content (Rea et al., 2002; Obrist et al., 2011; Blackwell & Driscoll, 2015; Yang et
80 al., 2018; Wohlgemuth et al., 2021). In polluted sites the soil is the main source of Hg to the vegetation while away
81 from those sites the atmosphere is the most important source (Naharro et al., 2018). The Hg source in foliage varies
82 with respect to the amount of contamination (Hanson et al., 1995).

83 The studies of the Hg cycle in forest ecosystems show that gaseous elemental Hg(0) is the main source taken up by
84 plants (Bishop et al. 2020; Zhou et al. 2021). Analysis of long term atmospheric Hg(0) and CO₂ concentrations are
85 very informative to understand the role of the vegetation in the global Hg cycle (Jiskra et al., 2018). Emission reduction
86 measures adopted in Europe and North America since the 70s are corroborated by Hg dendrochemistry analysis
87 showing a declining Hg concentration trend from the older to newer tree rings. Indeed, tree ring Hg
88 (dendrochronology) is a powerful archiving tool for atmospheric Hg(0). After Hg(0) oxidation inside the leaves, Hg(II)
89 bind to organic compounds and then is transported to the bole wood via the phloem (Beauford et al., 1977; Lindberg
90 et al., 1979). This is corroborated by the recent study of McLagan et al., (2022) showing the benefit of the stable Hg
91 isotope analysis on dendrochemistry. Several studies have evidenced seasonal variations of the atmospheric Hg(0)
92 contents (ie. in temperate Northern Hemisphere by Jiskra et al., 2018; in Western Mediterranean Basin in South Italy
93 (Martino et al. 2022) with high values in winter and low values in summer. Interestingly, Jiskra et al., (2018) show
94 also a significant positive correlation between the monthly Hg(0) and CO₂ concentrations. They highlighted a one-

95 month offset in Hg(0) summer time minima happening in September in comparison to the CO₂ minima value occurring
96 in August, this trend is not observed in winter time. The uptake of Hg(0) by the vegetation continues during CO₂
97 respiration periods during the fall and night when the ecosystem exchange of CO₂ turns from being a sink to becoming
98 a source (Wofsy et al., 1993; Jiskra et al., 2018).

99 The total gaseous Hg (TGM) in the Mediterranean atmosphere is similar to Northern Europe (1.3 to 2.4 ng m⁻³) (Kotnik
100 et al. 2014). In the case of a semi-closed sea such as the Mediterranean basin with warm summers, high sea-water
101 evaporation, solar radiations and Hg anthropogenic sources, the Mediterranean Sea acts as a net source of Hg to the
102 global atmosphere (Kotnik et al. 2014) making the Mediterranean an air-pollution emission area (Baayoun et al. 2019;
103 Borjac et al. 2019).

104 The olive tree (*Olea europaea* L.) is one of the most distinctive Mediterranean agro-ecosystems tree species (Besnard
105 et al., 2013), and is adapted to drought (Sghaier et al. 2019). Considered to be among the oldest trees in the
106 Mediterranean basin, centennial olive trees are still growing in many countries along both the eastern and western
107 shore, surviving numerous stresses and are of considerable historical, cultural and ecological importance (Terral et al.
108 2004). The olive tree still remains a key component of agriculture today and will be into the future. Therefore, genetic
109 characterization of olive varieties and genetic resources (Khadari et al., 2019; Galatali et al., 2021), description based
110 on morphological characters and phenology of growth stages of olive trees (Sanz-Cortés et al., 2002), experimentation
111 through field irrigation and/or more rarely through drought stress treatments (Alcaras et al., 2016) have been conducted
112 to avoid genetic erosion, optimize the water use for irrigation and hence improve orchard management, and solely to
113 better understand the biodiversity. Only few studies have focused on the response of the olive tree to Hg pollution in
114 its natural Mediterranean environment (Higueras et al., 2012; Higueras et al., 2016; Guarino et al., 2021; Labdaoui et
115 al., 2021).

116 Lebanon, a small country at the Eastern Mediterranean, is facing important anthropogenic pressure within a changing
117 environment (Gérard and Nehmé 2020). The air quality in Lebanon all over the country is noted to be moderately
118 unsafe with an annual mean concentration of 31 µg/m³ of PM_{2.5} (Particulate Matter) which is above the maximum
119 recommended value (10 µg/m³) (Lebanon: Air Pollution IAMAT 2020). Adding to that, soil samples collected from
120 different areas in southern Lebanon showed values of Hg concentration ranging between 160-6480 ng/g showing a
121 high contamination levels (Borjac et al. 2020) as indicated by World reference Senesil et al., 1999; Kabata-Pendias &
122 Pendias, 2000. The main contributors of the air pollution include cement industries, mineral and chemical factories,
123 vehicles emissions, food processing and oil refining. Ancient olive groves are found across different agroclimatic
124 areas at different altitudinal belts, still producing olives and oil for consumption with these various pollution pressures.
125 In this study two sites, known for their century-old olive groves and located at two different altitudes in Lebanon,
126 were selected to assess the Hg contents. In these remote areas, no direct sources of mercury contamination are reported
127 and hence we expect very low Hg concentrations. However, due to atmospheric transport of Hg, dry or wet deposition
128 of Hg can be expected in remote areas (Grigal, 2003). The main objectives of this study are to examine and compare
129 Hg levels in foliage, stems, fruits, litter and soil measured in each of these two olive groves, which we monitored
130 monthly for 18 months. The second objective is to analyze the relative importance of Hg uptake by the soil and foliage
131 in comparison with the atmospheric Hg. Since the distribution of Hg pollution is by nature geographically widespread,

132 and given the extent of Hg pollution in the Mediterranean and the transfer of pollution by wind and the Mediterranean
133 Sea, long-distance contamination occurs over large areas. This study may draw an adequate baseline for Eastern
134 Mediterranean and region of similar climates inventories on Hg vegetation uptake and new studies on olive trees in
135 the Mediterranean to reconstruct regional Hg pollution concentrations in the past and present.

136 **2. Materials and methods**

137
138 Two monumental olive groves were chosen in the context of their historical and agricultural importance,
139 since these two sites are considered to contain olive trees more than 1400 years old and are still productive.

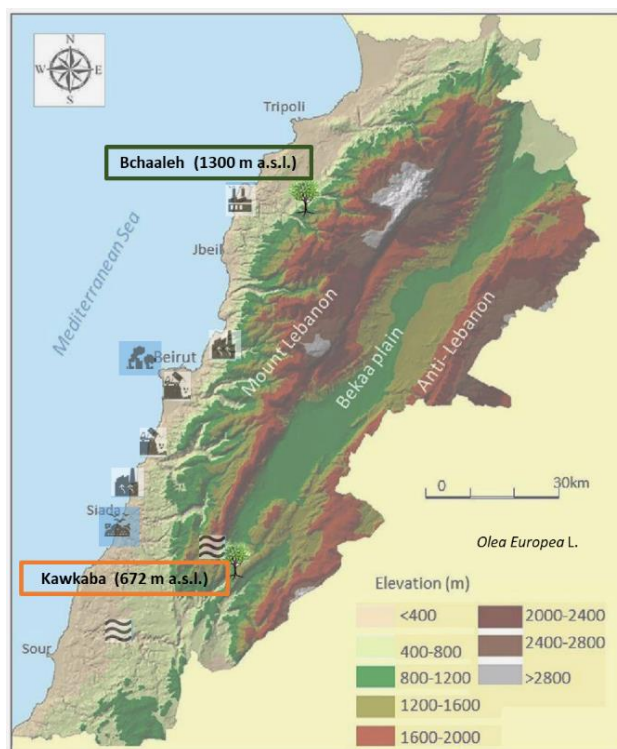
140 **2.1. Geographic setting and environmental context**

141 142 **2.1.1. Bchaaleh site - North Lebanon**

143
144 This grove is situated in Batroun district (Latitude 34°12'06'' N, Longitude 35°49'23'' E, Altitude 1300 m.a.s.l.)
145 (Figure 1). Olive trees are growing rainfed in a sandy loam texture soil of grain size analysis of sand, silt and clay
146 percentages are 52.8 %, 38.7 % and 10.7 % respectively. Soil pH is 7.07 ± 0.26 with organic matter and calcium
147 carbonate contents are 1.7 % and 38.3 % respectively (Yazbeck et al. 2018). In this study, soil profiles of carbon and
148 nitrogen contents were analyzed. Organic carbon contents decreased with soil depth from about 4 % at 0-1 cm (Soil
149 surface) to 2.7 % at 30-60 cm. The total nitrogen is about 0.3 % at 1cm depth and 0.2 % at 30-60 cm depth. The olive
150 trees are located on two terraces. The first terrace is at 1.5 meter above the road level while the second is at the road
151 level. They are maintained by the municipality for the last four decades as an endowment property. Precipitation
152 average ranges between 229 and 392 mm in winter and between zero and less than 2 mm/season in summer, while
153 average temperature is between 4 and 8 °C in winter and between 20 and 23 °C in summer and average relative
154 humidity of 63% (data extracted from LARI climatic data) (Table S1, Figure S1).

155 The village is at about 36 km from Chekka town located at a lower altitude (0-200 m.a.s.l.) nearby the sea (Figure 1),
156 and which is classified as a source of air pollution (EJOLT 2019). Chekka is the site of an important national cement
157 factory responsible of carbon dioxide, sulfur dioxide, nitrous oxides, carbon monoxide and particulate material
158 emissions causing respiratory and health issues (Kobrossi et al. 2002) and water pollution (Nassif et al. 2016). At 28
159 km from Bchaaleh, the small commercial port of Selaata (0-37 m.a.s.l.) emits many pollutants (ie. Phosphogypsum,
160 heavy metals, radionuclides) expanding via water and air pathways (Petrlik et al. 2013; Yammine et al. 2010). To our
161 knowledge no direct Hg pollution is reported at Chekka and Selaata sites. However a dissolved gaseous Hg from
162 natural and human activities is saturated in the upper Eastern Mediterranean Sea, Gårdfeldt et al., (2003) have
163 evidenced that Mediterranean Sea is a source of airborne elemental Hg.

164



165
 166 **Figure 1.** Site locations of the two selected focus areas (modified after Shared Water Resources of Lebanon, Nova
 167 Science Publishers 2017).
 168

169 **2.1.2. Kawkaba site - South Lebanon**
 170

171 The second grove is located in the village of Kawkaba, South Lebanon (Latitude 33°23'856'' N, Longitude
 172 35°38'588'' E, Altitude 672 m.a.s.l. (Figure 1). Kawkaba soil is characterized as clay loam soil of pH 7.5 ± 0.5 . Soil
 173 organic material and calcium carbonate average are 1.7 % and 59.0 % respectively (Al-Zubaidi et al., 2008) and grain
 174 size analysis of sand, silt and clay percentages are 6 %, 28 % and 66 % respectively. The analysis of organic carbon
 175 and nitrogen at the 0-1 cm and at 0-30 cm decrease from about 9.0 % to 2.2 % and from 0.9 % to 0.3 % for the carbon
 176 and nitrogen respectively. Average precipitation ranges between 215 and 374 mm in winter and drop to almost zero
 177 mm in summer, while average temperature is between 7 and 11 °C in winter and between 21 and 27 °C in summer
 178 and relative humidity of 61% (data extracted from LARI climatic data) (Table S1, Figure S1).

179 The village has to its east the Hasbani river, originated from the north-western slopes of Mount Hermon in Hasbaya
 180 (36 km away from Kawkaba and located at 750 m.a.s.l.) (Badr et al. 2014; Jurdi et al. 2002). On the other hand, the
 181 Litani River (170 km long and located at 800 to 1000 m.a.s.l) (Figure 1) rising in the south of the Bekaa valley is
 182 about 29 km away from Kawkaba (Abou Habib et al. 2015, Khatib et al. 2018). These two rivers are polluted and for
 183 these reasons they are not used for irrigating crops in Kawkaba and surrounding areas while the olive trees are growing
 184 rainfed as per indicated by the municipality of Kawkaba. Here as well, we did not find indication of direct Hg pollution.
 185 Climatic data in both Bchaaleh and Kawkaba were collected from meteorological station and manual rain gauge
 186 installed in the villages by LARI (Lebanese Agricultural Research Institute). CO₂ data used in this study are from
 187 NOAA Global Monitoring Laboratory (https://gml.noaa.gov/webdata/ccgg/trends/co2/co2_trend_gl.txt).

188 **2.2. Field sampling**

189
190 For the Hg concentration analysis, four olive trees (3-5 m in diameter and an average height of 4-6 m) were sampled
191 in each of the two groves from February 2019 to September 2020. Within Bchaaleh two trees were selected from the
192 upper terrace (BCO1-Bchaaleh-Tree 1, BCO4-Bchaaleh-Tree 4) and two other trees were sampled from a lower
193 terrace located 1.5 m below the upper one (BCO9-Bchaaleh-Tree 9, BCO12-Bchaaleh-Tree 12) (Figure S2). In
194 Kawkaba, four trees were selected and sampled (KWO1-Kawkaba-Tree 1, KWO2-Kawkaba-Tree 2, KWO3-
195 Kawkaba- Tree 3, KWO4-Kawkaba-Tree 4). For each olive tree, both sun exposed and shaded foliage and stems
196 (terminal portions of 20 cm) with no evidence of pathogens were randomly taken and merged from the upper, middle,
197 and lower canopy position of the olive trees on a monthly basis using a manual pruner. The phenological growth stages
198 of olive trees described by Sanz-Cortés et al.,(2002) in Spain suggest leaf development from March to November.
199 Hence it should be mentioned that the Hg concentration measured on monthly collected foliage represents an average
200 of Hg accumulated in young foliage (year N of collection where N is equal to 2019 and 2020) and older foliage (N-1
201 year and N-2 years). Fruits were collected in April 2019. Litter and soil surface were separately collected on the whole
202 top surface area of the olive groves and stored in different paper bags once every four months. In parallel, soil sampling
203 was performed using a bucket auger to a maximum depth of 60 cm. In both sites Bchaaleh and Kawkaba, the soil
204 showed uniform color and texture. Soil cores were fractioned in soil surface (0-1 cm), 0 to 30 cm depth and from 30
205 to 60 cm depth in order to study the effect and accumulation of Hg concentration on the different depth layers. To
206 avoid contamination, gloves were worn while collecting samples, and the equipment was rinsed with methanol
207 between every sample. A set of 453 samples were collected and stored in paper bags until further preparation for the
208 Hg analysis.

209

210 **2.3. Sample preparation for Hg analysis**

211
212 Collected foliage and stems were rinsed with distilled water and then dried for 48 hours in an oven at a temperature
213 of 50°C at maximum (Demers et al., 2013; Li et al., 2017; Pleijel et al., 2021). This procedure likely eliminate any
214 Hg(0) present in the samples. The dried foliage, stems, litter and olive fruits samples were grinded using an electrical
215 stainless grinding machine with no heating system for 5-10 minutes, while soil samples were prepared with a manual
216 natural agate grinder. All samples were later sieved using an inox stainless-steel 125-micron sieve mesh to collect
217 homogeneous powders for analysis. A total of 150 mg for foliage and soil (50 mg/analysis), and 300 mg of litter and
218 stems (100 mg/analysis) were considered in triplicates for analysis of Hg concentrations.

219

220 **2.4. Analytical method**

221
222 For the Hg elemental analysis, a total of 453 powder samples from foliage, stem, grain, litter and soil were analyzed
223 using an advanced Hg analyzer AMA 254 (Altec) as described elsewhere (Barre et al. 2018; Duval et al. 2020). A
224 known amount of sample (50-100 mg) is weight in a nickel boat, using a 10⁻⁶ g precision balance. The sample aliquot
225 is first dried at 120°C for 60s and subsequently pyrolyzed at 750°C for 150s, under oxygen flow. The resulting gaseous

226 Hg produced during the sample decomposition is amalgamated on a gold trap and then released to an Atomic
227 Absorption spectrometer after a thermal desorption step at 950°C. The AMA 254 instrument was calibrated through
228 several external matrix-matched calibration procedures using the following certified reference materials: IAEA-456
229 sediment (77 ± 5 ng Hg/g), NIST-1575A pine needles ($39,9 \pm 0,7$ ng Hg/g) and IAEA336 (200 ± 40 ng Hg/g). The
230 QA/QC evaluation of the analytical procedure was completed with a continuous monitoring of the blank's values
231 (Nickel boat Hg background noise), every 15 analyzed samples. The precision of the measurements was assessed
232 through replicated analyses (n=2) of 13 % of the total amount of samples (n=453). Average relative standard deviations
233 of 5 % and 2.5 % are thus associated to the reported Hg concentrations for the 2019 and 2020 samples batches,
234 respectively. The absolute detection limit (ADL) of the analytical technique (AMA 254) was estimated at 0.04 ng Hg.
235 As a consequence, the method detection limit (MDL) for samples analyzed were 0.7 ng Hg/g for soil, litter and foliage
236 and 0.4 ng Hg/g for stem and wood. These MDL were much lower than the measured Hg concentration in the various
237 samples.

238 Subsamples of soil were used for carbon and nitrogen elemental contents (%) analysis. A 2 mg (acid washed soil and
239 bulk soil) of powders were weighed into tin capsules and measured by dry combustion using a Pyrocube Elemental
240 Analyser (EA, Elementar GmbH).

241

242 **2.5. Statistical analysis**

243

244 For the statistical analysis we used the R 4.1.0 program. Our data are not normally distributed, so for the effect of
245 tissue type on Hg concentration, Wilcoxon test was used with the tissue type (foliage and stems) as the main effect.
246 Pearson correlation analysis was used to examine the inter-individual correlation of Hg concentration between the
247 trees. Correlation between Hg concentration of soil surface, litter and foliage was studied using a correlation test. For
248 the seasonal effect (Winter: Mid-December till Mid-March, Spring: Mid-March till Mid-June, Summer: Mid-June till
249 Mid-September, Autumn: Mid-September till Mid-December) on Hg concentration, Wilcoxon test was used
250 considering the unequal data available for the different seasons. Finally, the effect of climatic factors (Temperature,
251 precipitation, pCO₂) on Hg accumulation was examined using a Wilcoxon test.

252

253 **3. Results**

254

255 **3.1. Hg concentrations in plant tissues, litter and soil at Bchaaleh and Kawkaba groves**

256

257 Hg concentrations measured in the different sampled materials (plant tissues, litter and soil) varied generally according
258 to both tree tissues and groves agroclimatic conditions (Table 1). Hg values in the foliage varied significantly between
259 the two groves (p-value= $1.581 \cdot 10^{-6}$), where the highest concentration was recorded in Bchaaleh (48.1 ± 10.6 ng/g)
260 vs. (35 ± 12.4 ng/g) in Kawkaba. Soil surface also recorded a difference in Hg concentration between Bchaaleh and
261 Kawkaba, with 61.9 ± 20.0 ng/g in Bchaaleh and 128.5 ± 9.4 ng/g in Kawkaba. Soil 0-30 cm samples taken from
262 Bchaaleh and Kawkaba groves, values ranged between 31.8 ± 4.7 ng/g and 70.2 ± 23.4 ng/g respectively. In soil 30-
263 60 cm Hg concentrations recorded 19.5 ± 6.73 ng/g at Bchaaleh. No significant differences were recorded for litter

264 and stems Hg concentrations (p-value= 0.0915 and p-value=0.2215 respectively) between the groves, with litter values
 265 of 62.9 ± 17.8 at Bchaaleh and 75.7 ± 20.3 ng/g at Kawkaba vs. stem values of 7.9 ± 2.8 ng/g at Bchaaleh and $9.0 \pm$
 266 4.7 ng/g at Kawkaba. Positive correlations were observed between soil and litter in Bchaaleh ($r=0.60$) and Kawkaba
 267 ($r=0.95$) though statistically insignificant (p-value= 0.40 and 0.13 respectively).

268 The comparison between Bchaaleh and Kawkaba soil surface Hg contents showed significant difference between the
 269 two groves (p-value=0.04746). We observe the same significant difference when comparing the soil horizon of 0-30
 270 cm of both groves. In descending order of Hg concentrations and considering the different sites, plant tissue, soil and
 271 litter samples, the Hg concentrations could be ranked in Bchaaleh, soil surface > litter> foliage > soil 0-30 cm > soil
 272 30-60 cm > stems > fruits; and in Kawkaba, soil surface > litter > soil 0-30 > foliage > soil 30-60 > stems > fruits
 273 (Table 1).

274
 275 **Table 1.** Overall mean values of Hg concentration (ng/g) of the different studied material in both Bchaaleh and
 276 Kawkaba olive groves
 277

Sample material	Bchaaleh (BC)			Kawkaba (KW)		
	Average (ng/g)	SD	N	Average (ng/g)	SD	N
Foliage	48.1	10.6	66	35.0	12.4	67
Stems	7.9	2.8	66	9.0	4.7	67
Litter	62.9	17.8	7	75.7	20.3	6
Soil Surface	61.9	20.0	8	128.5	9.4	6
Soil 0-30cm	31.8	4.7	6	70.2	23.4	5
Soil 30-60cm	19.5	6.7	5	28.0		1
Fruits	7.0	3.5	3	11.0		1

278
 279 **3.2. Seasonal variation of Hg concentration in plant tissues, litter and soil**
 280

281 Hg concentrations recorded between February 2019 and September 2020 (Table 2) reflected a significant seasonal
 282 variation in both sites (p-value< 2.2×10^{-16})

283 In Bchaaleh grove, foliage registered its highest Hg concentration during winter and spring with 61.8 ± 7.6 ng/g and
 284 55.1 ± 12.5 ng/g respectively, and its lowest Hg amount during summer and autumn with 41.5 ± 12.7 ng/g and $44.4 \pm$
 285 6.2 ng/g, respectively. A seasonal effect on foliage and stems was registered (p-value< 2.2×10^{-16} ; Figure 2a,c). The
 286 stems and soil 0-30cm highest values was registered in autumn. Significant differences were found in foliage Hg
 287 values between summer and winter (p-value=0.00020), and autumn and winter (p-value= 0.00014). Similarly, stems
 288 Hg values varied significantly between spring and winter (p-value=0.030), autumn and winter (p-value=0.047). Litter
 289 highest Hg content occur in summer in Bchaaleh olive groves (79.3 ± 26.5 ng/g) and the lowest in winter (48.6 ± 13.3
 290 ng/g) (p-value = 0.2286). Highest Hg contents in the soil surface of Bchaaleh is recorded in summer (84.5 ± 21.2
 291 ng/g).

292 In Kawkaba, the highest Hg concentrations for foliage and stems were registered in spring with 51.8 ± 4.5 ng/g, 11.7
 293 ± 6.7 ng/g respectively (Table 2, Figure 2b,d). Significant differences were found in foliage Hg values between

294 summer and winter (p-value=0.013), autumn and winter (p-value= 0.00067), autumn and spring (p-value=1.589*10⁻
 295 ⁰⁵), spring and winter (p-value= 9.383*10⁻⁰⁵) and spring and summer (p-value=2.327*10⁻⁰⁶). Similarly, stem Hg values
 296 varied significantly between spring and winter (p-value=0.006), spring and summer (p-value=0.0036) and autumn and
 297 spring (p-value=0.011). There is no seasonal variation between the litter different seasons for Bchaaleh nor for
 298 Kawkaba. Bchaaleh and Kawkaba groves soil surface, 0-30 cm and 30-60cm Hg values varied significantly between
 299 seasons, (p-value < 0.05). A seasonal variation is observed in both olive groves especially in the foliage.

300
 301 **Table 2.** Seasonal mean Hg concentration (ng/g) and standard deviations of the different studied material in both
 302 Bchaaleh and Kawkaba olive groves. Grey color indicated the highest Hg concentration values among the different
 303 elements material during the different seasons.
 304

Hg (ng/g)												
Bchaaleh	Spring	SD	N	Summer	SD	N	Autumn	SD	N	Winter	SD	N
Foliage	55.1	12.5	16	41.5	12.7	24	44.4	6.2	12	61.8	7.6	18
Stems	7.8	3.8	16	7.61	3.9	24	8.3	2.7	12	6.4	2.9	18
Litter	79.3	26.5	3	64.7	4	4	55.5	3.54	2	48.6	13.3	3
Soil Surface	58.3	13	3	84.5	21.2	4	50		1	50.6	23.5	3
0-30cm	33.6	6.2	2	32.2	4.3	2	34.5	7.79	2	27	0.7	3
30-60cm	23.1	9.1	2	20.7	10.32	2	19.6	9.05	2	11		1
Kawkaba	Spring	SD	N	Summer	SD	N	Autumn	SD	N	Winter	SD	N
Foliage	51.8	4.5	16	28	7.2	24	28.5	7.2	16	33.9	5.6	18
Stems	11.7	6.7	16	6.5	1.4	24	7.7	2.1	16	6.9	1.6	18
Litter	90.1	29.3	2	67	24	2	70	1.4	2			
Soil Surface	132	8.5	2	118	4.2	2	135.6	2.2	2			
0-30cm	57.9	11.2	2	65.8		1	84.8	36.4	2			
30-60cm	28		1									

305
 306

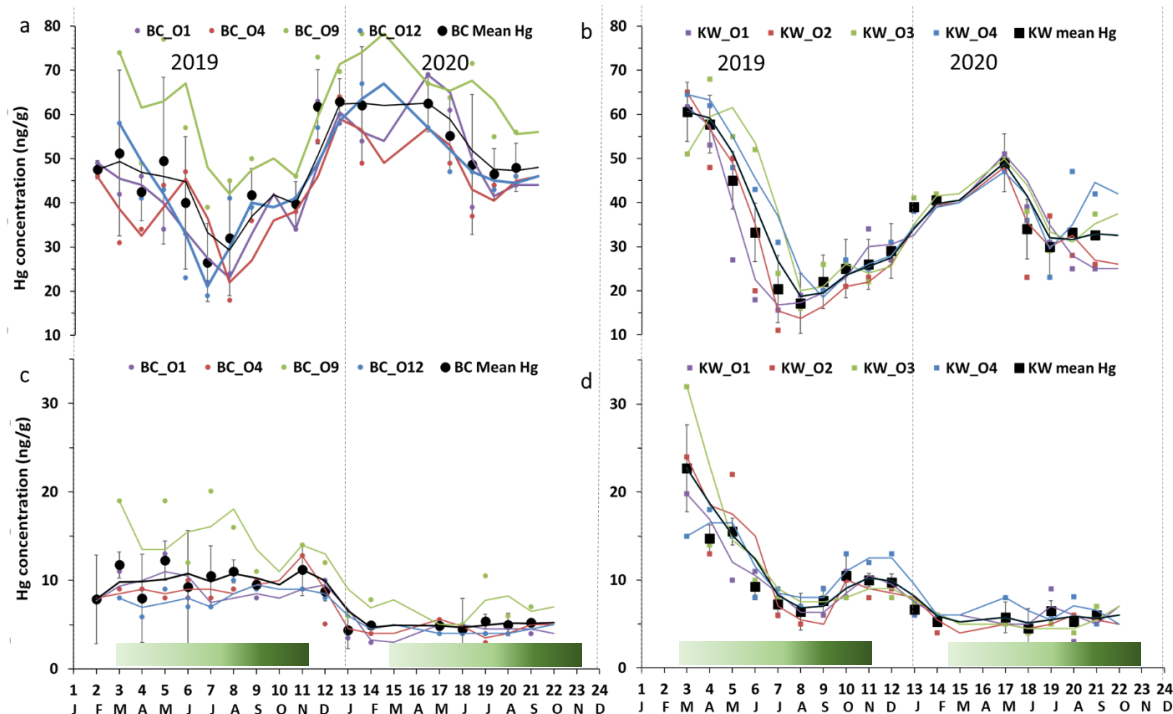


Figure 2. Seasonal variations of foliage Hg concentration in (a) Bchaaleh (BC) and (b) Kawkaba (KW) olive groves and stems Hg concentration in (c) Bchaaleh and (d) Kawkaba olive groves. Shaded green horizontal bars represent the leaf development of olive trees during the growing season of cultivars in Spain according to the BBCH scale (Sanz-Cortès et al., 2002).

3.3. Inter-individual variability between trees for each site

In the upper terrace of Bchaaleh grove, the foliage average Hg concentration of BCO4 and BCO1 varied between 42.4 ± 11.5 ng/g and 44.6 ± 13.3 ng/g respectively showing no significant difference (p -value = 0.8225). In the lower terrace of the same site, foliage average Hg concentrations of trees BCO12 and BCO9 were found to vary from 45.6 ± 12.7 ng/g to 60.7 ± 12.7 ng/g respectively (Figure 2a) exhibiting a significant difference (p -value=0.0059). Tree BCO9 is significantly different to each of the three trees (p -value< 0.0059) while BCO1, BCO4 and BCO12 have very similar Hg contents (p -value= 0.46).

In the upper terrace of Bchaaleh grove, the stems average Hg concentration of BCO4 and BCO1 varied between 7.0 ± 2.8 ng/g and 7.1 ± 2.9 ng/g respectively showing no significant difference (p -value= 0.94). In the lower terrace, stems average Hg concentrations of BCO12 and BCO9 are 6.4 ± 2.2 ng/g and 11.2 ± 5.2 ng/g respectively showing a significant difference (p -value= 0.0054; Figure 2c). For BCO1 and BCO12 there was no significance difference (p -value= 0.5725), the same goes for BCO4 and BCO12 (p -value= 0.523).

The average concentration per tree in foliage and stems were 32.4 ± 12.2 ng/g and 8.5 ± 4.0 ng/g respectively for KWO1, 32.8 ± 14.7 ng/g and 8.9 ± 6.0 ng/g for KWO2, 37.6 ± 14.0 ng/g and 9.3 ± 6.7 ng/g for KWO3 and 37.7 ± 13.6 ng/g and 9.6 ± 4.0 ng/g for KWO4 (Figure 2b,d). In Kawkaba grove, comparison of the foliage Hg concentration between the four studied trees shows no significant difference ($0.22 < p$ -value<1), neither for the stems ($0.21 < p$ -value<0.96).

332 **3.4. Hg concentration and agro-climatic effect**

333
334 At first glance, seasonal variations of the Hg concentrations of the foliage of both sites suggest a covariation with
335 climatic parameters (Precipitation amounts, Relative Humidity and Temperature) (Figure SI) and atmospheric pCO₂.
336 Foliage Hg content increased with higher precipitation and lower temperature (Autumn and Winter) while during the
337 warmer and dryer seasons (May to mid-October), the Hg concentration of foliage decreased (Figure SI). However, the
338 Wilcoxon test for a non-normal distribution shows no significant correlation between Hg concentration of foliage and
339 precipitation (p-value= 0.95). While temperature, relative humidity and atmospheric CO₂ (pCO₂) shows a significant
340 correlation (p-value = $2.2e^{-16}$). For the stems, Hg concentration also showed no significant correlation with
341 precipitation (p-value=0.1147), and a significant correlation with temperature, relative humidity and pCO₂ (p-value=
342 $2.2e^{-16}$).

343 **4. Discussion**

344 345 **4.1. Hg concentration in plant tissues, soil and litter in the studied groves**

346
347 In both groves our values showed a higher Hg concentration in the olive foliage (Bchaaleh average of 48.1 ± 10.6
348 ng/g; Kawkaba average of 35.0 ± 12.4 ng/g), than that of the stems (Bchaaleh average of 7.9 ± 2.8 ng/g; Kawkaba
349 average of 9.0 ± 4.7 ng/g) and that of olive fruits (7 ± 3.5 ng/g at Bchaaleh, n=3 and 11 ng/g in Kawkaba, n=1). Our
350 data corroborates previous studies (Bargagli 1995; Higuera et al. 2016) showing that olive foliage has the highest Hg
351 concentration of plant tissues. Our values are lower than 200 ng/g considered as Hg pollution threshold (Kabata-
352 Pendias & Pendias, 2000) and implying no pollution effect for both Bchaaleh and Kawkaba groves (Table S2; Figure
353 S3a,b). This suggests that our sites are good remote bioindicators of the uptake of Hg through the plant, although more
354 prolonged time range study is needed. However, in an overview of vegetation uptake of mercury and impacts on global
355 cycling, Zhou et al., (2021) suggested lower values for unpolluted sites (litterfall 43 ng/g > foliage 20 ng/g and branch
356 12 ng/g). Knowing that our sites correspond to unpolluted areas of Lebanon, the lower values of Zhou et al., (2021)
357 obtained from an ensemble of various species (trees and grasses) and not specifically on olive trees, we considered
358 that the threshold value of 200 ng/g (Kabata-Pendias and Pendias 2000) is more adapted to our comparison.

359 As described in several studies, Hg in foliage originates predominantly from the atmospheric gaseous Hg(0) through
360 stomatal uptake (Ericksen et al., 2003; Lindberg et al., 1979; Zhou et al., 2021). Adding to that, the atmospheric Hg
361 uptake in foliage exceeds Hg stomatal re-emission (Pleijel et al., 2021; Zhou et al., 2021). Inside the leaves the oxidized
362 Hg(II) has high affinities to bind covalently with organic groups (Du & Fang, 1983; Clarkson & Magos, 2006; Pleijel
363 et al., 2021). The Hg can be translocated by phloem transport to the stems and eventually into roots and potential
364 release into soils may also be contributing to Hg accumulation in soils (Giesler et al., 2017; Schaefer et al., 2020).

365 The soil surface and litter registered the highest Hg concentration (62 to 129 ng/g) among all samples (foliage, stems,
366 fruit) in both groves (Table 1) suggesting that the soil is the main Hg reservoir through the Hg throughfall and litter
367 inputs (Tomiya et al., 2005). Our findings are in agreement with studies on evergreen forest ecosystems reporting
368 that soil can hold more than 60 % of Hg input to the forest floor (Wang et al. 2016). Our soil surface sites values (61.9
369 ± 20.0 ng/g in Bchaaleh and 128.5 ± 9.4 ng/g in Kawkaba) show higher Hg concentration in Kawkaba compared to

370 the general background level of Hg as defined by uncontaminated soil world reference mean Hg contents (20 to 100
371 ng/g; Kabata-Pendias and Pendias 2000; Senesil et al. 1999; Gworek et al. 2020). However, both sites have
372 significantly lower values compared to known industrial and mining contaminated sites (> 1000 ng/g ;). Nevertheless,
373 studies conducted in different sites show a wide range of natural background Hg levels (ie. topsoils in Europe, India,
374 Brazil, Norwegian Arctic, New Zealand have values of 40, 50, 80, 110, 230 ng/g respectively) (Gworek et al. 2020)
375 making it difficult to set a specific Hg threshold value for uncontaminated soil (Table S2; Figure S3c). Due to the
376 differences registered in different countries and sites of sampled soil, this indicates a link with chemical and
377 mineralogical soil properties (ie. pH, humic acid, soil grain size distribution, organic matter type and clay percentage)
378 affecting Hg in soil and its transport (Richardson et al., 2013; Chen et al., 2016; O'Connor et al., 2019). Nitrogen can
379 also be a factor affecting the Hg content in soil depending on its characteristics. Nitrogen increase can change the
380 equilibrium of soil solution and the morphology of roots, causing a possible increase in Hg availability in soil and
381 increases the Hg uptake by the plant (Alloway, 1995; Barber, 1995; Carrasco-Gil et al., 2012). The increase in Hg
382 availability in the soil is due to the organic Nitrogen that provides a high absorption capacity, retaining the atmospheric
383 Hg deposition (Obrist et al., 2009). Nitrogen supply prevents oxidative stress in roots, but also can improve root
384 development and increase the uptake of Hg from the soil (Carrasco-Gil et al. 2012). Hence, we suggest that lower
385 values in Bchaaleh soils are likely explained by the low clay, organic carbon and nitrogen contents (10.7 %, 4 % and
386 0.3 % in soil surface respectively). While Kawkaba higher Hg soil contents can be explained by the higher clay
387 proportion (66 %) and organic carbon and nitrogen contents (9 % and 0.92 %). On such clay loam soils and rich
388 organic matter, Hg binding is facilitated explaining higher content (O'Connor et al. 2019).

389 The litter showed higher Hg concentration than that in foliage in both Bchaaleh (62.9 ± 17.8 ng/g) and Kawkaba (75.7
390 ± 20.3 ng/g) (Table 1). This has been also described by Rea et al., (1996) and Zhou et al., (2021) in uncontaminated
391 and contaminated sites where litterfall Hg contents were systematically higher than the foliage Hg contents. The
392 bacterial and chemical decomposition of the litter decrease significantly the amount of C compared to the Hg that
393 conversely may continue to increase due to the continued absorption of Hg from precipitation and throughfall (Obrist
394 et al., 2011; Pokharel & Obrist, 2011; Zhou et al., 2021). Another possible explanation is that the leaves shed as litter
395 are likely to mostly be the oldest leaves which have accumulated Hg during the longest period of time and thus have
396 higher Hg concentrations than the remaining foliage have on average since they consist of both younger and older
397 foliage (Rea et al. 1996; Pleijel et al. 2021).

398

399 **4.2. Seasonal foliage Hg content versus seasonal atmospheric Hg and CO₂**

400

401 The late winter-early spring registered the highest Hg concentration for foliage in both groves, while summer and
402 early fall to a less extent recorded the lowest concentrations. This seasonal change is explained by the seasonal tree
403 physiology variations such as the Hg accumulation in leaves after stomatal uptake (Pleijel et al., 2021; Wohlgemuth
404 et al., 2021). We can suggest that during winter-early spring, water is available and photosynthetic activity is not
405 limited, hence both CO₂ and Hg diffuse through opened stomata inside the foliage. As shown on figure 2, Hg in foliage
406 is low in summer-fall and hence act as a sink of Hg. ~~Note that despite we mixed three generations of olive leaves (year~~
407 ~~N to N-3), the most recent of which are known to be low in mercury~~ **A clear seasonal pattern of Hg concentration in**

408 foliage is evident, despite being based on three generation of olive leaves (1-3 years old), with youngest leaves known
409 to have low concentrations (Pleijel et al., 2021), the seasonal signal is still very remarkable. Therefore, one can
410 speculate that the mercury levels would have been higher if we had avoided the recently formed foliage during spring
411 and early summer. This may also explain the large difference in Hg levels between litter and foliage.

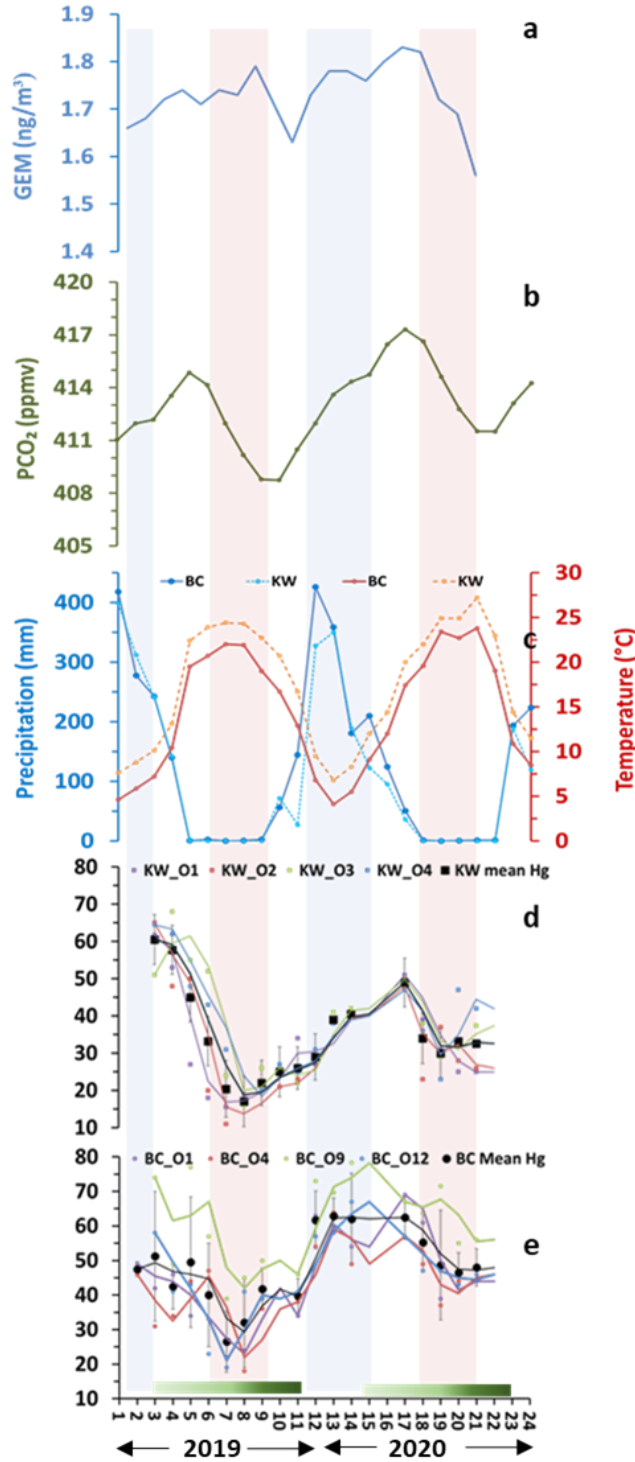
412 ~~At our latitudes, Bchaaleh and Kawkaba foliage evergreen olive trees show~~ Evergreen olive foliage at our sites show
413 a decrease in Hg contents from end of March to late August, with minimum values centered in August suggesting a
414 decline of the plant Hg uptake likely explained by the reduction of the stomatal conductance (Lindberg et al., 2007;
415 Pleijel et al., 2021). This minimal photosynthetic activity occurs during the driest season (0 mm precipitation) and
416 hottest temperatures (above 25°C) at our sites. ~~Year 2020 has higher foliage Hg values than 2019. This can be related~~
417 ~~to a higher vegetation uptake in 2020 in comparison to 2019. Martino et al., (2022) showed seasonal variability of~~
418 ~~Gaseous Elemental Mercury (GEM) in the atmosphere in southern Italy (Figure 3a). They also related this seasonality~~
419 ~~to high energy use for heat during winter thus higher emissions due to coal combustion (Weigelt et al., 2015) and the~~
420 ~~effect of air mass trajectory on the GEM seasonality where the winter peak is connected to the Hg re-emission from~~
421 ~~sea surface and with long range transport, in addition to the GEM oxidation rate in warmer months (Horowitz et al.,~~
422 ~~2017; Martino et al., 2022). For the period 2018-2020, Martino et al. (2022) showed an atmospheric GEM~~
423 ~~depletion when NDVI values increased (normalized difference vegetation index). This can explain the lower foliage~~
424 ~~Hg content in 2019 compared to 2020 at our study sites in Lebanon. Martino et al. (2022) comparing the normalized~~
425 ~~difference vegetation index values (NDVI) with GEM concentration of the same seasons over the different years (2018~~
426 ~~to 2020), show that the higher vegetation uptake explains the GEM depletion in certain seasons and years. This was~~
427 ~~also collaborating Jiskra et al., (2018) for the Northern Hemisphere site. Since no data of atmospheric mercury in~~
428 ~~Lebanon or surrounding countries are available we used the atmospheric Hg time series data of Martino et al. (2022)~~
429 ~~(Figure 3a). We observed opposite trends between foliage Hg concentration and air Hg (negative covariation in 2019~~
430 ~~and positive covariation in 2020) (Figure a,d,e).~~

431 Alternatively other studies reported a positive correlation between atmospheric Hg and crops (Niu et al. 2011) as
432 observed in our study between the Hg_{foliage} and the atmospheric Hg in 2020 (Figure 3a,d,e). This suggest the hypothesis
433 where our groves seasonally exposed to high atmospheric Hg, accumulate Hg in their foliage (Lindberg et al. 2007;
434 Pleijel et al. 2021). According to Hanson et al. (1995), a compensation point for Hg uptake by plant foliage can be
435 considered but no information to our knowledge is available for the specific case of the olive trees. The tight link
436 between foliage Hg uptake and stomatal conductance seasonal variations can be also deduced from the analysis of the
437 partial pressure of the pCO_{2atm} seasonal variation (Obrist, 2007; Jiskra et al., 2018; Obrist et al., 2018; Pleijel et al.,
438 2021) (Figure 3b,d,e). Very good covariation between olive foliage Hg and pCO_{2atm} are shown for Bchaaleh and
439 Kawkaba despite a notable offset of one month at Kawkaba to two months at Bchaaleh can be deduced (Figure S4).

440 Taking into account our calculated time lags, we obtained significant correlations between our foliage Hg content and
441 pCO_{2atm} of 0.718 and 0.704 in Bchaaleh and Kawkaba respectively. Interestingly a one month time-lag between
442 atmospheric Hg and pCO_{2atm} is also reported by Jiskra et al. (2018) for most northern hemisphere sites. The offset of
443 one to two months between maxima of Bchaaleh and Kawkaba foliage Hg (March/April) and pCO_{2atm} (May) suggests
444 that the minimum of Hg in the foliage occur during the decreasing phase of the pCO_{2atm} when the global northern

445 hemisphere tend to become a net sink of CO₂. When minimum values of pCO_{2atm} are reached at the end of the dry
446 summer (Figure 3b), concomitant to minimum atmospheric Hg (Figure 3a), end of the drought and increase of
447 precipitation (Figure 3c), Bchaleh and Kawkaba olive trees show a recovery in the Hg uptake rates. The photosynthetic
448 activity and the stomatal conductance related to the climatic parameters (temperature, precipitation, humidity, pCO₂)
449 as shown by Ozturk et al. (2021) and the atmospheric Hg explain our foliage Hg seasonal cycle. At a regional scale,
450 our sites show different time lags between Bchaaleh and Kawkaba that we cannot explain fully except their altitudinal
451 differences, which can suggest that Bchaaleh grove benefits of less drought in summer. ~~During the day the evaporation
452 increase and the plant water content decreases and become minimal during midday, noting that the soil water content
453 is high. During the evening the olive tree seeks soil water as an equilibrium. If soil water is not available enough to
454 cover the olive need, the evergreen olive is able to adapt through conservation of internal water especially during
455 severe summer drought, due to its ability to restrict water loss to the atmosphere and maximize extraction of soil water
456 (Connor & Fereres, 2010). Taking into account Hg results obtained during several seasonal campaigns in the surface
457 waters of the Mediterranean Sea and the above atmospheric layer, it has been evidenced that the highest Hg fluxes to
458 the atmosphere occur mainly in summer (Wangberg et al. 2001; Kotnik et al. 2014). Moreover, a higher total gaseous
459 mercury (TGM) is registered in the eastern Mediterranean compared with the western Mediterranean and Northern
460 Europe (Wangberg et al., 2001). Olive trees are known to be a mycotrophic plant. Mycorrhiza acts as a barrier that
461 restrict the movement of heavy metals from the roots to the plants (Wu et al., 2016; Riaz et al., 2021). In the
462 Mediterranean region, it is reported that intensity of mycorrhizal colonization of olive tree roots increases with the
463 increase of seasonal precipitation/decrease in temperature and decreased with the increase of air temperature, when it
464 is drier (Meddad Hamza et al., 2017). This confirms that in the decrease of mycorrhizal activity in summer, a possible
465 minimal Hg uptake from the soil and roots to the foliage and stems through water during the drought season may
466 occur (Rea et al., 2002; Meddad Hamza et al., 2017). Further analysis and data are necessary to confirm the above
467 assumption.~~

468



469
470

471 **Figure 3.** Seasonal variations of (a) atmospheric Hg(0) (Martino et al. 2022), (b) pCO₂ (NOAA Global Monitoring
472 Laboratory), (c) precipitations and temperature of Bchaaleh and Kawkaba respectively and (d) and (e) foliage Hg
473 concentration in Bchaaleh and Kawkaba olive groves respectively. Shaded green horizontal bars represent the leaf
474 development of olive trees during the growing season of cultivars in Spain according to the BBCH scale (Sanz-Cortès
475 et al., 2002). Shaded colored lines correspond to the Winter (Blue) and Summer (Red).

476 **4.3. Hg cycling in the stems, litter and soil system**

477
478 For each site, Hg contents in stems exhibit a narrow range between the different trees except tree BCO9, which had
479 the highest stem values. We speculate that this higher Hg content is the adjunction of chemical products as fertilizer
480 on the plot 549 belonging to a different owner (Figure S2) likely between fall and winter. It was observed by (Zhao &
481 Wang, 2010) that the fertilizer used and its source of phosphorous may affect the Hg content in the product and thus
482 affect the amount of Hg transported into the fertilized soil.

483 At a seasonal scale, the averaged Hg values of soil system show ~~statistical significance difference~~ statistically
484 significant differences between the four seasons, while stems show statistically significant differences significant
485 difference between winter (lowest values) and spring (p-value= 0.030) and winter-autumn (p-value= 0.047) in
486 Bchaaleh grove mostly similar to foliage changes. While litter shows no significant difference between seasons. The
487 same behavior was registered in Kawkaba in litter and soils, while stems showing statistical significance differences
488 between autumn and spring (p-value= 0.011), spring-winter (p-value= 0.006) and spring-summer (p-value= 0.004)
489 (Table 2). Despite the small amount of Hg content in the stems, the statistically significant seasonal changes may
490 suggest that small amount of Hg move from the foliage to the lignified tissues as stems. However, we cannot neglect
491 the Hg transport in xylem sap from the roots to the aboveground plant tissues even if minimal (Yang et al. 2018).

492 We can suggest the following Hg cycling in the system of the olive grove/soil. In winter-early spring the highest
493 concentrations in foliage continuously feed the litter and can explain the following maximal spring Hg content of the
494 litter. The decomposition of the litter organic matter during the wettest conditions likely liberate Hg in the Hg(0) or
495 Hg(II) forms or MeHg either towards the atmosphere or the surface soil (see Table 2) respectively (Gworek et al.,
496 2020). A fraction of the degraded organic matter is transferred through gaseous evaporative processes towards the
497 atmosphere while another fraction of the Hg is leaching towards the deeper soil in addition to dry Hg deposition during
498 dry season (Teixeira et al. 2017). We can also speculate that the small Hg decrease observed in soil 0-30, 30-60 cm
499 during the winter season in Bchaaleh can be due to the minimal absorption of total Hg and MeHg through the roots
500 and xylem sap to the above ground tissues (Johnson and Lindberg 1995).

501 **5. Conclusion**

502
503 This is the first study conducted on monumental olive trees in a-remote site of the MENA region without local
504 contamination and followed at a monthly basis over 18 months. Findings of our study indicate a higher uptake of Hg
505 in the olive foliage compared to stems, fruits items and a remarkable Hg_{Foliage} seasonal variation in both studied groves.
506 Winter and Spring were particularly suitable for Hg accumulation in foliage in both sites. The significant correlation
507 between our Hg_{Foliage} contents and the atmospheric Hg content and pCO_2 , despite the one to two months' time lag,
508 suggests that the main source of Hg_{Foliage} is the atmospheric Hg as observed in different species and studies (conifers
509 and hardwood). Hg is absorbed by the foliage, via the open stomata, driven by the interaction of high vegetal activity,
510 temperature, water availability and the processes that control transpiration, which is likely to be seasonal. Hence
511 physiological and climatic processes explain the seasonal Hg accumulation in foliage. Thus, a more intensive study
512 taking account the phenological dynamics of olive tree foliage must be focused on. Further comparison and studies
513 on the seasonal atmospheric Hg in the eastern Mediterranean basin are necessary to test our hypothesis of the reversed

514 seasonality of Hg in 2019 and positive covariation in 2020 since contrary to the global Northern Hemisphere and
515 western Mediterranean region vegetation, our olive groves act as a sink of Hg and CO₂ when global Northern and
516 western Mediterranean vegetation is emitting. This relationship $Hg_{\text{Foliage}} - Hg_{\text{atm}} - pCO_{2\text{atm}}$ should be further investigated
517 along the season and locally to better understand the observed time lags. Soil surface registered the highest Hg
518 concentration among all studied compartments due to well-known processes of litter and throughfall that incorporate
519 Hg to the soil surface. Moreover, this study highlights significant differences between Hg_{soil} in Bchaaleh and Kawkaba
520 groves due to differences in soil characteristics. In this study we worked on the present time samples in order to have
521 a better understanding of the Hg cycle in the olive tree. Our main contribution in this study is to see how the present-
522 day olive trees records some elements such as Hg to better understand how the Hg in tree rings could be used for the
523 past accumulation records.

524

525 **Data availability**

526 The datasets generated during and/or analyzed during the current study are available from the corresponding author
527 on reasonable request.

528

529 **Author Contributions**

530 The corresponding author **Ilham Bentaleb** is responsible for ensuring that the descriptions are accurate and agreed upon
531 by all authors. Conceptualization and methodology were done and developed by **Ilham Bentaleb** and **Lamis Chalak**.
532 The material collection was performed by **Naghm Tabaja, Ilham Bentaleb, Lamis Chalak, Ihab Jomaa, and Milad**
533 **Riachy**. Sample storage and preparation in Lebanon organized by **Naghm Tabaja**. Material preparation at ISEM by
534 **Naghm Tabaja**, Data collection and analysis were performed by Naghm Tabaja, **Ilham Bentaleb, David Amouroux,**
535 **and Emmanuel Tessier**. The setting of the meteorological stations by **Ihab Jomaa**. Subsamples of soil were analyzed
536 for carbon and nitrogen elemental contents (%) by **François Fourel**. The first draft of the manuscript was written by
537 **Naghm Tabaja, Ilham Bentaleb, Lamis Chalak, David Amouroux, Ihab Jomaa, and Milad Riachy** commented
538 on previous versions of the manuscript. All authors read and approved the final manuscript. Supervision was done by
539 Ilham Bentaleb and Lamis Chalak.

540

541

542 **Competing interests**

543 The authors declare that they have no known competing financial interests or personal relationships that could have
544 appeared to influence the work reported in this paper.

545

546

547 **Acknowledgments**

548 The authors would like to acknowledge the National Council for Scientific Research of Lebanon (CNRS-L) and
549 Montpellier University for granting a doctoral fellowship (CNRS-L/UM) to Naghm Tabaja. The authors would also
550 like to thank the Franco-Lebanese Hubert Curien Partnership (PHC-CEDRE) project 44559PL for the funding
551 provided. Institute of Evolutionary Science of Montpellier (ISEM) at Montpellier University and the Research
552 Platform for Environment and Science- Doctoral School of Science and Technology (PRASE-EDST) at the Lebanese
553 University are also acknowledged for their support of the laboratory work. Credits go to the Lebanese Agriculture
554 Research Institute (LARI) for assuring automated weather stations and manual rain gauges per site. The authors are
555 grateful to the Municipality of Bchaaleh (Mr. Rachid Geagea) and the Municipality of Kawkaba (Ms. Mira Khoury).
556 Acknowledgments are extended to Ms. Amira Yousef at LARI for her kind support and to Mr. Akram Tabaja for
557 helping during fieldwork. We are very grateful to Pleijel Hakan who reviewed this article improving significantly our
558 paper. We deeply acknowledge Andrew Johnston for the English revision.

559 **Funding**

560 This work was supported and funded by Lebanon and Montpellier University (CNRS-L/UM grant), and PHC-
561 CEDRE-project 44559PL

562

563 **References**

564

565 Abou Habib, N., Taleb, M., & Khoury, R.: Environmental and social safeguard studies for lake qaraoun pollution
566 prevention project. V1(E4749), 2015.

567 Alcaras, L. M. A., Rousseaux, M. C., & Searles, P. S.: Responses of several soil and plant indicators to post-harvest
568 regulated deficit irrigation in olive trees and their potential for irrigation scheduling. *Agricultural Water
569 Management*, 171, 10–20. <https://doi.org/10.1016/j.agwat.2016.03.006>, 2016.

570 Alloway, B. J.: *Heavy Metals in Soils*. Springer Science & Business Media, 1995.

571 Al-Zubaidi, A., Yanni, S., & Bashour, I.: Potassium status in some Lebanese soils. *Lebanese Science Journal*, 9(1),
572 81–97, 2008.

573 Assad, M.: Transfert des éléments traces métalliques vers les végétaux: Mécanismes et évaluations des risques dans
574 des environnements exposés à des activités anthropiques. 218, 2017.

575 Baayoun, A., Itani, W., El Helou, J., Halabi, L., Medlej, S., El Malki, M., Moukhadder, A., Aboujaoude, L. K.,
576 Kabakian, V., Mounajed, H., Mokalled, T., Shihadeh, A., Lakkis, I., & Saliba, N. A.: Emission inventory of
577 key sources of air pollution in Lebanon. *Atmospheric Environment*, 215, 116871.
578 <https://doi.org/10.1016/j.atmosenv.2019.116871>, 2019.

579 Badr, R., Holail, H., & Olama, Z.: Water quality assessment of hasbani river in south lebanon: microbiological and
580 chemical characteristics and their impact on the ecosystem. 3, 16, 2014.

581 Barber, S. A.: *Soil Nutrient Bioavailability: A Mechanistic Approach*. John Wiley & Sons, 1995.

582 Bargagli, R.: The elemental composition of vegetation and the possible incidence of soil contamination of samples.
583 *Science of The Total Environment*, 176(1–3), 121–128. [https://doi.org/10.1016/0048-9697\(95\)04838-3](https://doi.org/10.1016/0048-9697(95)04838-3),
584 1995.

585 Barre, J. P. G., Deletraz, G., Sola-Larrañaga, C., Santamaria, J. M., Bérail, S., Donard, O. F. X., & Amouroux, D.:
586 Multi-element isotopic signature (C, N, Pb, Hg) in epiphytic lichens to discriminate atmospheric
587 contamination as a function of land-use characteristics (Pyrénées-Atlantiques, SW France). *Environmental
588 Pollution*, 243, 961–971. <https://doi.org/10.1016/j.envpol.2018.09.003>, 2018.

589 Beauford, W., Barber, J., & Barringer, A. R.: Uptake and Distribution of Mercury within Higher Plants. *Physiologia*
590 *Plantarum*, 39(4), 261–265. <https://doi.org/10.1111/j.1399-3054.1977.tb01880.x>, 1977.

591 Besnard, G., Khadari, B., Navascues, M., Fernandez-Mazuecos, M., Bakkali, A. E., Arrigo, N., Baali-Cherif, D., de
592 Caraffa, V. B.-B., Santoni, S., Vargas, P., & Savolainen, V.: The complex history of the olive tree: From
593 Late Quaternary diversification of Mediterranean lineages to primary domestication in the northern Levant.
594 *Proceedings of the Royal Society B: Biological Sciences*, 280(1756), 20122833–20122833, 2013.

595 Bishop, K. H., Lee, Y.-H., Munthe, J., & Dambrine, E.: Xylem sap as a pathway for total mercury and
596 methylmercury transport from soils to tree canopy in the boreal forest. *Biogeochemistry*, 40, 101–113,
597 1998.

598 Bishop, K., Shanley, J. B., Riscassi, A., de Wit, H. A., Eklöf, K., Meng, B., Mitchell, C., Osterwalder, S., Schuster,
599 P. F., Webster, J., & Zhu, W.: Recent advances in understanding and measurement of mercury in the
600 environment: Terrestrial Hg cycling. *Science of The Total Environment*, 721, 137647.
601 <https://doi.org/10.1016/j.scitotenv.2020.137647>, 2020.

602 Blackwell, B. D., & Driscoll, C. T.: Using foliar and forest floor mercury concentrations to assess spatial patterns of
603 mercury deposition. *Environmental Pollution*, 202, 126–134. <https://doi.org/10.1016/j.envpol.2015.02.036>,
604 2015.

605 Boening, D. W.: Ecological effects, transport, and fate of mercury: A general review. 17, 2000.

606 Borjac, J., El Joumaa, M., Kawach, R., Youssef, L., & Blake, D. A.: Heavy metals and organic compounds
607 contamination in leachates collected from Deir Kanoun Ras El Ain dump and its adjacent canal in South
608 Lebanon. *Heliyon*, 5(8), e02212. <https://doi.org/10.1016/j.heliyon.2019.e02212>, 2019.

609 Borjac, J., El Joumaa, M., Youssef, L., Kawach, R., & Blake, D. A.: Quantitative Analysis of Heavy Metals and
610 Organic Compounds in Soil from Deir Kanoun Ras El Ain Dump, Lebanon. *The Scientific World Journal*,
611 2020, 1–10. <https://doi.org/10.1155/2020/8151676>, 2020.

612 Briffa, J., Sinagra, E., & Blundell, R.: Heavy metal pollution in the environment and their toxicological effects on
613 humans. *Heliyon*, 6(9), e04691. <https://doi.org/10.1016/j.heliyon.2020.e04691>, 2020.

614 Carrasco-Gil, S., Estebarez-Yuberob, M., Medel-Cuestab, D., Millán, R., & Hernández, L. E.: Influence of nitrate
615 fertilization on Hg uptake and oxidative stress parameters in alfalfa plants cultivated in a Hg-polluted soil.
616 *Environmental and Experimental Botany*, 75. <https://doi.org/10.1016/j.envexpbot.2011.08.013>, 2012.

617 Cavallini, A., Natali, L., Durante, M., & Maserti, B. (1999). Mercury uptake, distribution and DNA affinity in
618 durum wheat (*Triticum durum* Desf.) plants. *Science of The Total Environment*, 243–244, 119–127.
619 [https://doi.org/10.1016/S0048-9697\(99\)00367-8](https://doi.org/10.1016/S0048-9697(99)00367-8).

620 Chen, X., Ji, H., Yang, W., Zhu, B., & Ding, H. Speciation and distribution of mercury in soils around gold mines
621 located upstream of Miyun Reservoir, Beijing, China. *Journal of Geochemical Exploration*, 163, 1–9.
622 <https://doi.org/10.1016/j.gexplo.2016.01.015>, 2016.

623 Clarkson, T. W., & Magos, L.: The Toxicology of Mercury and Its Chemical Compounds. *Critical Reviews in*
624 *Toxicology*, 36(8), 609–662. <https://doi.org/10.1080/10408440600845619>, 2006.

625 Dastoor, A., Angot, H., Bieser, J., Christensen, J. H., Douglas, T. A., Heimbürger-Boavida, L.-E., Jiskra, M., Mason,
626 R. P., McLagan, D. S., Obrist, D., Outridge, P. M., Petrova, M. V., Ryjkov, A., St. Pierre, K. A., Schartup,
627 A. T., Soerensen, A. L., Toyota, K., Travnikov, O., Wilson, S. J., & Zdanowicz, C.: Arctic mercury
628 cycling. *Nature Reviews Earth & Environment*, 3(4), Article 4. [https://doi.org/10.1038/s43017-022-00269-](https://doi.org/10.1038/s43017-022-00269-w)
629 [w](https://doi.org/10.1038/s43017-022-00269-w), 2022.

630 Demers, J. D., Blum, J. D., & Zak, D. R.: Mercury isotopes in a forested ecosystem: Implications for air-surface
631 exchange dynamics and the global mercury cycle: Mercury isotopes in a forested ecosystem. *Global*
632 *Biogeochemical Cycles*, 27(1), 222–238. <https://doi.org/10.1002/gbc.20021>, 2013.

633 Du, S.-H., & Fang, S. C.: Catalase activity of C3 and C4 species and its relationship to mercury vapor uptake.
634 *Environmental and Experimental Botany*, 23(4), 347–353. [https://doi.org/10.1016/0098-8472\(83\)90009-6](https://doi.org/10.1016/0098-8472(83)90009-6),
635 1983.

636 Duval, B., Gredilla, A., Fdez-Ortiz de Vallejuelo, S., Tessier, E., Amouroux, D., & de Diego, A.: A simple
637 determination of trace mercury concentrations in natural waters using dispersive Micro-Solid phase
638 extraction preconcentration based on functionalized graphene nanosheets. *Microchemical Journal*, 154,
639 104549. <https://doi.org/10.1016/j.microc.2019.104549>, 2020.

640 EJOLT: Cimenterie Nationale Factory in Chekaa, Lebanon | EJAtlas. *Environmental Justice Atlas*.
641 <https://ejatlas.org/conflict/chekaa>, Acces date: 2019.

642 Ericksen, J. A., Gustin, M. S., Schorran, D. E., Johnson, D. W., Lindberg, S. E., & Coleman, J. S.: Accumulation of
643 atmospheric mercury in forest foliage. *Atmospheric Environment*, 37(12), 1613–1622.
644 [https://doi.org/10.1016/S1352-2310\(03\)00008-6](https://doi.org/10.1016/S1352-2310(03)00008-6), 2003.

645 Ermolin, M. S., Fedotov, P. S., Malik, N. A., & Karandashev, V. K.: Nanoparticles of volcanic ash as a carrier for
646 toxic elements on the global scale. *Chemosphere*, 200, 16–22.
647 <https://doi.org/10.1016/j.chemosphere.2018.02.089>, 2018.

648 Freeman, M., & Carlson, R. M.: Essential nutrients. *Olive Production Manual*, 3353, 75, 2005.

649 Friedli, H. R., Arellano, A. F., Cinnirella, S., & Pirrone, N.: Initial Estimates of Mercury Emissions to the
650 Atmosphere from Global Biomass Burning. *Environmental Science & Technology*, 43(10), 3507–3513.
651 <https://doi.org/10.1021/es802703g>, 2009.

652 Galatali, S., A., N., & Kaya, E.: Characterization of Olive (*Olea Europaea* L.) Genetic Resources via PCR-Based
653 Molecular Marker Systems. 2, 26–33. <https://doi.org/10.24018/ejbio.2021.2.1.146>, 2021.

654 Gårdfeldt, K., Sommar, J., Ferrara, R., Ceccarini, C., Lanzillotta, E., Munthe, J., Wängberg, I., Lindqvist, O.,
655 Pirrone, N., Sprovieri, F., Pesenti, E., & Strömberg, D.: Evasion of mercury from coastal and open waters
656 of the Atlantic Ocean and the Mediterranean Sea. *Atmospheric Environment*, 37, 73–84.
657 [https://doi.org/10.1016/S1352-2310\(03\)00238-3](https://doi.org/10.1016/S1352-2310(03)00238-3), 2003.

658 Gérard, J., & Nehmé, C.: Lebanon. Méditerranée. *Revue Géographique Des Pays Méditerranéens / Journal of*
659 *Mediterranean Geography*, 131, Article 131. <https://journals.openedition.org/mediterranee/11018#>, 2020.

660 Giesler, R., Clemmensen, K. E., Wardle, D. A., Klaminder, J., & Bindler, R.: Boreal Forests Sequester Large
661 Amounts of Mercury over Millennial Time Scales in the Absence of Wildfire. *Environmental Science &*
662 *Technology*, 51(5), 2621–2627. <https://doi.org/10.1021/acs.est.6b06369>, 2017.

663 Grigal, D.: Mercury Sequestration in Forests and Peatlands: A Review. *Journal of Environmental Quality - J*
664 *ENVIRON QUAL*, 32. <https://doi.org/10.2134/jeq2003.0393>, 2003.

665 Guarino, F., Improta, G., Triassi, M., Castiglione, S., & Cicatelli, A.: Air quality biomonitoring through *Olea*
666 *europaea* L.: The study case of “Land of pyres.” *Chemosphere*, 282, 131052.
667 <https://doi.org/10.1016/j.chemosphere.2021.131052>, 2021.

668 Gworek, B., Dmuchowski, W., & Baczewska-Dąbrowska, A. H.: Mercury in the terrestrial environment: A review.
669 *Environmental Sciences Europe*, 32(1), 128. <https://doi.org/10.1186/s12302-020-00401-x>, 2020.

670 Hanson, P. J., Lindberg, S. E., Tabberer, T. A., Owens, J. G., & Kim, K.-H.: Foliar exchange of mercury vapor:
671 Evidence for a compensation point. *Water, Air, & Soil Pollution*, 80(1–4), 373–382.
672 <https://doi.org/10.1007/BF01189687>, 1995.

673 Higuera, P., Amorós, J. A., Esbrí, J. M., García-Navarro, F. J., Pérez de los Reyes, C., & Moreno, G.: Time and
674 space variations in mercury and other trace element contents in olive tree leaves from the Almadén Hg-
675 mining district. *Journal of Geochemical Exploration*, 123, 143–151.
676 <https://doi.org/10.1016/j.gexplo.2012.04.012>, 2012.

677 Higuera, P. L., Amorós, J. Á., Esbrí, J. M., Pérez-de-los-Reyes, C., López-Berdonces, M. A., & García-Navarro, F.
678 J.: Mercury transfer from soil to olive trees. A comparison of three different contaminated sites.
679 *Environmental Science and Pollution Research*, 23(7), 6055–6061. [https://doi.org/10.1007/s11356-015-](https://doi.org/10.1007/s11356-015-4357-2)
680 [4357-2](https://doi.org/10.1007/s11356-015-4357-2), 2016.

681 Jindrich Petrik, Kodeih, N., IndyACT, Arnika Association, & IPEN WG.: Mercury in Fish and Hair Samples from
682 Batroun, Lebanon. <https://doi.org/10.13140/RG.2.2.12052.40327>, 2013.

683 Jiskra, M., Sonke, J. E., Obrist, D., Bieser, J., Ebinghaus, R., Myhre, C. L., Pfaffhuber, K. A., Wängberg, I.,
684 Kyllönen, K., Worthy, D., Martin, L. G., Labuschagne, C., Mkololo, T., Ramonet, M., Magand, O., &
685 Dommergue, A.: A vegetation control on seasonal variations in global atmospheric mercury concentrations.
686 *Nature Geoscience*, 11(4), 244–250. <https://doi.org/10.1038/s41561-018-0078-8>, 2018.

687 Johnson, & Lindberg: The biogeochemical cycling of Hg in forests: Alternative methods for quantifying total
688 deposition and soil emission. 1995, 80: 1069–1077, 9, 1995.

689 Jurdi, M., Korfali, S. I., Karahagopian, Y., & Davies, B. E.: Evaluation of Water Quality of the Qaraaoun Reservoir,
690 Lebanon: Suitability for Multipurpose Usage. 77(11–30), 20, 2002.

691 Kabata-Pendias, A., & Pendias, H.: Trace elements in soils and plants (3rd ed). CRC Press, 2000.

692 Khadari, B., El Bakkali, A., Essalouh, L., Tollon, C., Pinatel, C., & Besnard, G.: Cultivated Olive Diversification at
693 Local and Regional Scales: Evidence From the Genetic Characterization of French Genetic Resources.
694 *Frontiers in Plant Science*, 10. <https://www.frontiersin.org/articles/10.3389/fpls.2019.01593>, 2019.

695 Kobrossi, R., Nuwayhid, I., Sibai, A. M., El-Fadel, M., & Khogali, M.: Respiratory health effects of industrial air
696 pollution on children in North Lebanon. *International Journal of Environmental Health Research*, 12(3),
697 205–220. <https://doi.org/10.1080/09603/202/000000970>, 2002.

698 Kotnik, J., Sprovieri, F., Ogrinc, N., Horvat, M., & Pirrone, N.: Mercury in the Mediterranean, part I: Spatial and
699 temporal trends. *Environmental Science and Pollution Research*, 21(6), 4063–4080.
700 <https://doi.org/10.1007/s11356-013-2378-2>, 2014.

701 Labdaoui, D., Lotmani, B., & Aguedal, H.: Assessment of Metal Pollution on the Cultivation of Olive Trees in the
702 Petrochemical Industrial Zone of Arzew (Algeria). *South Asian Journal of Experimental Biology*, 11(3),
703 Article 3. [https://doi.org/10.38150/sajeb.11\(3\).p227-233](https://doi.org/10.38150/sajeb.11(3).p227-233), 2021.

704 Lebanon: Air Pollution | IAMAT: <https://www.iamat.org/country/lebanon/risk/air-pollution>, 2020

705 Li, D., Fang, K., Li, Y., Chen, D., Liu, X., Dong, Z., Zhou, F., Guo, G., Shi, F., Xu, C., & Li, Y.: Climate, intrinsic
706 water-use efficiency and tree growth over the past 150 years in humid subtropical China. *PLOS ONE*,
707 12(2), e0172045. <https://doi.org/10.1371/journal.pone.0172045>, 2017.

708 Li, R., Wu, H., Ding, J., Fu, W., Gan, L., & Li, Y.: Mercury pollution in vegetables, grains and soils from areas
709 surrounding coal-fired power plants. *Scientific Reports*, 7(1), 46545. <https://doi.org/10.1038/srep46545>,
710 2017.

711 Lindberg, S., Bullock, R., Ebinghaus, R., Engstrom, D., Feng, X., Fitzgerald, W., Pirrone, N., Prestbo, E., &
712 Seigneur, C.: A Synthesis of Progress and Uncertainties in Attributing the Sources of Mercury in
713 Deposition. *Ambio*, 36(1), 19–32, 2007.

714 Lindberg, S. E., Jackson, D. R., Huckabee, J. W., Janzen, S. A., Levin, M. J., & Lund, J. R.: Atmospheric Emission
715 and Plant Uptake of Mercury from Agricultural Soils near the Almadén Mercury Mine. *Journal of*
716 *Environmental Quality*, 8(4), 572–578. <https://doi.org/10.2134/jeq1979.00472425000800040026x>, 1979

717 Lodenius, M., Tulisalo, E., & Soltanpour-Gargari, A.: Exchange of mercury between atmosphere and vegetation
718 under contaminated conditions. *Science of The Total Environment*, 304(1–3), 169–174.
719 [https://doi.org/10.1016/S0048-9697\(02\)00566-1](https://doi.org/10.1016/S0048-9697(02)00566-1), 2003.

720 Luo, Y., Duan, L., Driscoll, C. T., Xu, G., Shao, M., Taylor, M., Wang, S., & Hao, J.: Foliage/atmosphere exchange
721 of mercury in a subtropical coniferous forest in south China. *Journal of Geophysical Research:*
722 *Biogeosciences*, 121(7), 2006–2016. <https://doi.org/10.1002/2016JG003388>, 2016.

723 Maillard, F., Girardclos, O., Assad, M., Zappellini, C., Pérez Mena, J. M., Yung, L., Guyeux, C., Chrétien, S.,
724 Bigham, G., Cosio, C., & Chalot, M.: Dendrochemical assessment of mercury releases from a pond and
725 dredged-sediment landfill impacted by a chlor-alkali plant. *Environmental Research*, 148, 122–126.
726 <https://doi.org/10.1016/j.envres.2016.03.034>, 2016.

727 McLagan, D. S., Biester, H., Navrátil, T., Kraemer, S. M., & Schwab, L.: Internal tree cycling and atmospheric
728 archiving of mercury: Examination with concentration and stable isotope analyses. *Biogeosciences*, 19, 4415–4429,
729 2022. <https://doi.org/10.5194/bg-19-4415-2022>, 2022.

730 McLagan, D. S., Stupple, G. W., Darlington, A., Hayden, K., Steffen, A., & Kamp, L.: Where there is smoke there is
731 mercury: Assessing boreal forest fire mercury emissions using aircraft and highlighting uncertainties
732 associated with upscaling emissions estimates. *Atmos. Chem. Phys.*, 19, 2021.

733 Naharro, R., Esbri, J., Amorós, J., & Higuera, P.: Atmospheric mercury uptake and desorption from olive-tree
734 leaves. *EGU2018-2982,2018*, 2, 2018

735 Nassif, N., Jaoude, L. A., El Hage, M., & Robinson, C. A.: Data Exploration and Reconnaissance to Identify Ocean
736 Phenomena: A Guide for <i>In Situ</i> Data Collection. *Journal of Water Resource and*
737 *Protection*, 08(10), 929–943. <https://doi.org/10.4236/jwarp.2016.810076>, 2016.

738 Niu, Z., Zhang, X., Wang, Z., & Ci, Z.: Field controlled experiments of mercury accumulation in crops from air and
739 soil. *Environmental Pollution*, 159(10), 2684–2689. <https://doi.org/10.1016/j.envpol.2011.05.029>

740 Obrist, D.: Atmospheric mercury pollution due to losses of terrestrial carbon pools? *Biogeochemistry*, 85(2), 119–
741 123. <https://doi.org/10.1007/s10533-007-9108-0>, 2011, 2007

742 Obrist, D., Johnson, D. W., & Lindberg, S. E.: Mercury concentrations and pools in four Sierra Nevada forest sites,
743 and relationships to organic carbon and nitrogen. 13, 2009.

744 Obrist, D., Kirk, J. L., Zhang, L., Sunderland, E. M., Jiskra, M., & Selin, N. E.: A review of global environmental
745 mercury processes in response to human and natural perturbations: Changes of emissions, climate, and land
746 use. *Ambio*, 47(2), 116–140. <https://doi.org/10.1007/s13280-017-1004-9>, 2018.

747 Obrist, M. K., Rathey, E., Bontadina, F., Martinoli, A., Conedera, M., Christe, P., & Moretti, M.: Response of bat
748 species to sylvo-pastoral abandonment. *Forest Ecology and Management*, 261(3), 789–798.
749 <https://doi.org/10.1016/j.foreco.2010.12.010>, 2011.

750 O’Connor, D., Hou, D., Ok, Y. S., Mulder, J., Duan, L., Wu, Q., Wang, S., Tack, F. M. G., & Rinklebe, J.: Mercury
751 speciation, transformation, and transportation in soils, atmospheric flux, and implications for risk
752 management: A critical review. *Environment International*, 126, 747–761.
753 <https://doi.org/10.1016/j.envint.2019.03.019>, 2019.

754 Ozturk, M., Altay, V., Gönenç, T. M., Unal, B. T., Efe, R., Akçiçek, E., & Bukhari, A.: An Overview of Olive
755 Cultivation in Turkey: Botanical Features, Eco-Physiology and Phytochemical Aspects. *Agronomy*, 11(2),
756 295. <https://doi.org/10.3390/agronomy11020295>, 2021.

757 Patra, M., & Sharma, A.: Mercury toxicity in plants. *The Botanical Review*, 66(3), 379–422.
758 <https://doi.org/10.1007/BF02868923>, 2000

759 Pleijel, H., Klingberg, J., Nerentorp, M., Broberg, M. C., Nyirambangutse, B., Munthe, J., & Wallin, G.: Mercury
760 accumulation in leaves of different plant types – the significance of tissue age and specific leaf area. *Biogeosciences*,
761 18, 6313–6328, 2021. <https://doi.org/10.5194/bg-18-6313-2021>, 2021.

762 Pokharel, A. K., & Obrist, D.: Fate of mercury in tree litter during decomposition. *Biogeosciences*, 8(9), 2507–2521.
763 <https://doi.org/10.5194/bg-8-2507-2011>, 2011.

764 Rea, A. W., Keeler, G. J., & Scherbatskoy, T.: The deposition of mercury in throughfall and litterfall in the lake
765 champlain watershed: A short-term study. *Atmospheric Environment*, 30(19), 3257–3263.
766 [https://doi.org/10.1016/1352-2310\(96\)00087-8](https://doi.org/10.1016/1352-2310(96)00087-8), 1996.

767 Rea, A. W., Lindberg, S. E., Scherbatskoy, T., & Keeler, G. J.: Mercury Accumulation in Foliage over Time in Two
768 Northern Mixed-Hardwood Forests. 19, 2002

769 Richardson, J. B., Friedland, A. J., Engerbretson, T. R., Kaste, J. M., & Jackson, B. P.: Spatial and vertical
770 distribution of mercury in upland forest soils across the northeastern United States. *Environmental*
771 *Pollution (Barking, Essex : 1987)*, 182, 127–134. <https://doi.org/10.1016/j.envpol.2013.07.011>, 2013.

772 Sanz-Cortés, F., Martínez-Calvo, J., Badenes, M. L., Bleiholder, H., Hack, H., Llacer, G., & Meier, U.: Phenological
773 growth stages of olive trees (*Olea europaea*). *Annals of Applied Biology*, 140(2), 151–157.
774 <https://doi.org/10.1111/j.1744-7348.2002.tb00167.x>, 2002.

775 Schaefer, K., Elshorbany, Y., Jafarov, E., Schuster, P. F., Striegl, R. G., Wickland, K. P., & Sunderland, E. M.:
776 Potential impacts of mercury released from thawing permafrost. *Nature Communications*, 11(1), Article 1.
777 <https://doi.org/10.1038/s41467-020-18398-5>, 2020.

778 Schneider, L., Allen, K., Walker, M., Morgan, C., & Haberle, S.: Using Tree Rings to Track Atmospheric Mercury
779 Pollution in Australia: The Legacy of Mining in Tasmania. *Environmental Science & Technology*, 53(10),
780 5697–5706. <https://doi.org/10.1021/acs.est.8b06712>, 2019.

781 Schwesig, D., & Krebs, O.: The role of ground vegetation in the uptake of mercury and methylmercury in a forest
782 ecosystem. *Plant and Soil*, 11, 2003.

783 Senesil, G. S., Baldassarre, G., Senesi, N., & Radina, B.: Trace element inputs into soils by anthropogenic activities
784 and implications for human health. *Chemosphere*, 39(2), 343–377. [https://doi.org/10.1016/S0045-](https://doi.org/10.1016/S0045-6535(99)00115-0)
785 [6535\(99\)00115-0](https://doi.org/10.1016/S0045-6535(99)00115-0), 1999.

786 Sghaier, A., Perttunen, J., Sievaänen, R., Boujnah, D., Ouessar, M., Ben Ayed, R., & Naggaz, K.: Photosynthetic
787 activity modelisation of olive trees growing under drought conditions. *Scientific Reports*, 9(1), 15536.
788 <https://doi.org/10.1038/s41598-019-52094-9>, 2019.

789 Teixeira, D. C., Lacerda, L. D., & Silva-Filho, E. V.: Mercury sequestration by rainforests: The influence of
790 microclimate and different successional stages. *Chemosphere*, 168, 1186–1193.
791 <https://doi.org/10.1016/j.chemosphere.2016.10.081>, 2017.

792 Terral, J.-F., Alonso, N., Capdevila, R. B. i, Chatti, N., Fabre, L., Fiorentino, G., Marinval, P., Jordá, G. P., Pradat,
793 B., Rovira, N., & Alibert, P.: Historical biogeography of olive domestication (*Olea europaea* L.) as revealed
794 by geometrical morphometry applied to biological and archaeological material: Historical biogeography of
795 olive domestication (*Olea europaea* L.). *Journal of Biogeography*, 31(1), 63–77.
796 <https://doi.org/10.1046/j.0305-0270.2003.01019.x>, 2004

797 Tomiyasu, T., Matsuo, T., Miyamoto, J., Imura, R., Anazawa, K., & Sakamoto, H.: Low level mercury uptake by
798 plants from natural environments—Mercury distribution in *Solidago altissima* L.-. *Environmental Sciences:*
799 *An International Journal of Environmental Physiology and Toxicology*, 12(4), 231–238, 2005.

800 UNEP: Technical Background Report to the Global Mercury Assessment 2018. IVL Svenska Miljöinstitutet, 2019.

801 Wang, X., Lin, C.-J., Lu, Z., Zhang, H., Zhang, Y., & Feng, X.: Enhanced accumulation and storage of mercury on
802 subtropical evergreen forest floor: Implications on mercury budget in global forest ecosystems: Hg storage
803 on subtropical forest floor. *Journal of Geophysical Research: Biogeosciences*, 121(8), 2096–2109.
804 <https://doi.org/10.1002/2016JG003446>, 2016.

805 Wofsy, S. C., Goulden, M. L., Munger, J. W., Fan, S.-M., Bakwin, P. S., Daube, B. C., Bassow, S. L., & Bazzaz, F.
806 A.: Net Exchange of CO₂ in a Mid-Latitude Forest. *Science*, 260(5112), 1314–1317.
807 <https://doi.org/10.1126/science.260.5112.1314>, 1993.

808 Wohlgemuth, L., Rautio, P., Ahrends, B., Russ, A., Vesterdal, L., Waldner, P., Timmermann, V., Eickenscheidt, N.,
809 Frst, A., Greve, M., Roskams, P., Thimonier, A., Nicolas, M., Kowalska, A., Ingerslev, M., Meril, P.,
810 Benham, S., Iacoban, C., Hoch, G., ... Jiskra, M.: Physiological and climate controls on foliar mercury
811 uptake by European tree species. *Biogeosciences*, 19, 1335–1353, 2022. [https://doi.org/10.5194/bg-19-](https://doi.org/10.5194/bg-19-1335-2022)
812 [1335-2022](https://doi.org/10.5194/bg-19-1335-2022), 2021.

813 Wright, L. P., Zhang, L., & Marsik, F. J.: Overview of mercury dry deposition, litterfall, and throughfall studies.
814 *Atmospheric Chemistry and Physics*, 16(21), 13399–13416. <https://doi.org/10.5194/acp-16-13399-2016>,
815 2016.

816 Yammine, P., Kfoury, A., El-Khoury, B., Nouali, H., El-Nakat, H., Ledoux, F., Courcot, D., & Aboukas, A.: A
817 preliminary evaluation of the inorganic chemical composition of atmospheric tsp in the selaata region,
818 north lebanon. *Lebanese Science Journal*, 11(1), 18, 2010.

819 Yanai, R. D., Yang, Y., Wild, A. D., Smith, K. T., & Driscoll, C. T.: New Approaches to Understand Mercury in
820 Trees: Radial and Longitudinal Patterns of Mercury in Tree Rings and Genetic Control of Mercury in
821 Maple Sap. *Water, Air, & Soil Pollution*, 231(5), 248. <https://doi.org/10.1007/s11270-020-04601-2>, 2020

822 Yang, Y., Yanai, R. D., Driscoll, C. T., Montesdeoca, M., & Smith, K. T.: Concentrations and content of mercury in
823 bark, wood, and leaves in hardwoods and conifers in four forested sites in the northeastern USA. *PLOS*
824 *ONE*, 13(4), e0196293. <https://doi.org/10.1371/journal.pone.0196293>, 2018.

825 Yazbeck, E. B., Rizk, G. A., Hassoun, G., El-Khoury, R., & Geagea, L.: Ecological characterization of ancient olive
826 trees in Lebanon- Bshaaleh area and their age estimation. 11(2 Ver. 1), 35–44, 2018.

827 Zhao, X., & Wang, D.: Mercury in some chemical fertilizers and the effect of calcium superphosphate on mercury
828 uptake by corn seedlings (*Zea mays* L.). *Journal of Environmental Sciences*, 22(8), 1184–1188.
829 [https://doi.org/10.1016/S1001-0742\(09\)60236-9](https://doi.org/10.1016/S1001-0742(09)60236-9), 2010

830 Zhou, J., Obrist, D., Dastoor, A., Jiskra, M., & Ryjkov, A.: Vegetation uptake of mercury and impacts on global
831 cycling. *Nature Reviews Earth & Environment*, 2(4), 269–284. [https://doi.org/10.1038/s43017-021-00146-](https://doi.org/10.1038/s43017-021-00146-y)
832 [y](https://doi.org/10.1038/s43017-021-00146-y), 2021

833 Zhou, J., Wang, Z., & Zhang, X.: Deposition and Fate of Mercury in Litterfall, Litter, and Soil in Coniferous and
834 Broad-Leaved Forests. *Journal of Geophysical Research: Biogeosciences*, 123(8), 2590–2603.
835 <https://doi.org/10.1029/2018JG004415>, 2018.